

1. INTRODUCTION

Hydroxyapatite is the dominant inorganic phase in natural bone. Synthetic hydroxyapatite particles, films, coatings, fibers and porous skeletons are used extensively in various biomedical applications. This bioceramic, $\text{Ca}_{10}(\text{PO}_4)_6(\text{OH})_2$, can be synthesized by many wet chemical and mechano-chemical methods. The sol-gel route is becoming a unique low-temperature technique to produce ultra fine and pure ceramic powders. Recently, hydroxyapatite powders and coatings have been successfully synthesized by the sol gel method. The process parameters have been optimized to produce high purity hydroxyapatite.

Porous calcium phosphate based scaffolds are used in a wide range of applications in tissue engineering, controlled drug delivery systems and in the treatment of bone disease. Various methods have been developed to introduce porosity in calcium phosphate scaffolds including incorporation of volatile organic particles, gel casting, replication of a polymer sponge or reticulation and salt leaching. A more recent approach to developing ceramic fibers and porous structures is the use of electrospinning. In this case, the inorganic solution that acts as a precursor to the ceramic (*e.g.* sol) may be mixed with a polymer solution and the mixture is electrospun at voltages between 10 to 30 kV. Several researchers have used electrospinning for the production of micro-porous ceramic structures containing a network of submicron fibers. A variety of ceramic fibers, with average diameters in the sub-micron range, have been produced by this technique. Typically, the sol is electrospun with a polymer solution and the resultant structure is calcined at temperatures on the order of 600°C to remove the polymer.

During electrospinning, the breakup of solution jets into droplets and fibers is strongly influenced by rheological properties of the solution. The molecular weights (M_w) of the polymer and concentration (c) have significant influences on solution rheology. In

particular, M_w plays a vital role in controlling solution viscosity. In this work, the feasibility of producing hydroxyapatite fibrous networks by calcination of an electrospun polymer-sol mixture has been studied. The effects of polymer molecular weight and of the volume fraction of the inorganic sol on the structures obtained after calcination have been examined.

2. LITERATURE REVIEW

2.1 Sol-gel Synthesis of Hydroxyapatite

Sintered calcium phosphate ceramics based on hydroxyapatite (HA, $\text{Ca}_{10}(\text{PO}_4)_6(\text{OH})_2$) or β -tricalcium phosphate (β -TCP, $\text{Ca}_3(\text{PO}_4)_2$) are one of the most prominent materials used in the treatment of orthopedic defects. They are also being used by many researchers for bone tissue engineering. Their chemical composition is highly related to the mineral phase of natural bone [1-3]. These similarities lead to a good biocompatibility between these materials and bone. Synthetic hydroxyapatite (HA) particles, films, coatings, fibers and porous skeletons are used extensively in several biomedical applications [4,5].

Traditionally, this bioceramic, $\text{Ca}_{10}(\text{PO}_4)_6(\text{OH})_2$, can be synthesized by solid state reactions, plasma techniques[6], hydrothermal hotpressing [7], and many wet chemical precipitation and mechano-chemical methods [8,9]. In wet precipitation method, the chemical reactions take place between calcium and phosphorus ions under a controlled pH and temperature of the solution. The precipitated powder is typically calcined at high temperature in order to obtain a stoichiometric apatitic structure. Slow titration and diluted solutions must be used to improve chemical homogeneity and stoichiometry within the system. Careful control of the solution condition is also required in the wet precipitation methods. In early reports, the decrease of solution pH below about 9 could lead to the formation of Ca-deficient apatite structure. In some cases, a well-crystallized HA phase was only developed while approaching a calcination temperature of 1200°C.

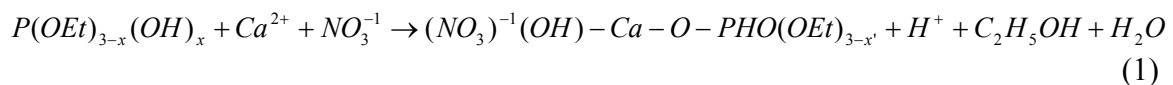
The sol-gel approach provides significantly easier conditions for the synthesis of HA. Sol-gel synthesis of HA ceramics has recently attracted much attention. Sol-gel process refers to a low-temperature method using chemical precursors that can produce ceramics and glasses with better purity and homogeneity [10]. This process is becoming a common technique to produce ultra fine and pure ceramic powders, fibers, coatings, thin films, and porous membranes. Compare to the conventional methods, the most attractive features and advantages of sol-gel process include (a) molecular-level homogeneity can be easily achieved through the mixing of two liquids; (b) the homogeneous mixture containing all the components in the correct stoichiometry ensures a much higher purity; and, (c) much lower heat treatment temperature to form glass or polycrystalline ceramics is usually achieved without resorting to a high temperature. More recently, the sol-gel method has been extensively developed and used in biotechnology applications [11].

2.1.1 Precursors

In the sol-gel synthesis of HA, a stoichiometric ratio of 1.67 between calcium and phosphorus precursors is required to achieve the accurate molar ratio of the final product. A number of combinations between calcium and phosphorus precursors were employed for sol-gel HA synthesis [15-18]. For example, Gross *et al.* [15] used calcium diethoxide and triethylphosphate to form pure HA phase at temperatures above 600°C. Jilavenkatesa *et al.* [16] used calcium acetate and triethyl phosphate as the precursors. Brendel *et al.* [17] obtained HA with poor crystallinity using calcium nitrate and phenyl dichlorophosphite as precursors. Lopatin *et al.* [18] used a hydrated solution of *N*-butyl acid phosphate mixed with calcium nitrate tetrahydrate dissolved in 2- methoxyethanol to

synthesize HA. Weng *et al.* [21] synthesized HA using a mixed ethanol solution of calcium nitrate and phosphorus pentoxide.

The chemical activity of the precursors is an important factor because of the slow reaction between Ca and P in the sol phase [12]. Haddow *et al.* [19] used calcium acetate together with a series of phosphorus precursors including phosphoric acid, phosphorus pentoxide, and triethyl phosphite. They found that the final product prepared from triethyl phosphite and calcium acetate showed the best wetting characteristic. Although phosphorus alkoxides have frequently been used as the phosphorus precursors for sol-gel HA synthesis, triethyl phosphate and triethyl phosphite are becoming the major materials used to prepare the precursors. The hydrolysis activity of the triethyl phosphate is relatively poor and a higher solution temperature together with a prolonged time period (of several days) is needed to form the HA phase [16]. Even if triethyl phosphite has higher activity, Gross *et al.* [15] reported in order to obtain HA, a reaction time as long as 24 hr is still required for triethyl phosphite to interact with the calcium precursor. Chai *et al.* [20] compared two calcium precursors, namely calcium diethoxide and calcium propionate, which reacted with triethyl phosphite to form HA coating. They found that the HA phase appeared only for calcium propionate solution. No HA formed when calcium ethoxide was used. In most of the reports, calcium nitrite is used to prepare the calcium precursor [12,13,17,18,21]. The simplified and idealized form of the chemical reaction between Ca and P is described below. But few detailed studies of the chemical pathways have been reported in the literature.



2.1.2 Aging Effect

In recent reports of the sol-gel procedure to synthesize hydroxyapatite, appropriate aging time and temperature of the precursor solution has been found to be two critical factors in developing the apatitic phase. Appropriate aging is required to complete the chemical reaction between calcium and phosphorus precursors. During the chemical reaction between calcium and phosphorus precursors, an intermediate compound is formed. This compound determines the resulting apatite phase after calcination. A preparation time of 24 hr or longer is generally reported in literature as required to form a desirable intermediate compound. Cai *et al.* [14] aged the sol at room temperature for as long as a week. The X-Ray diffraction (XRD) patterns are shown in Fig. 1.

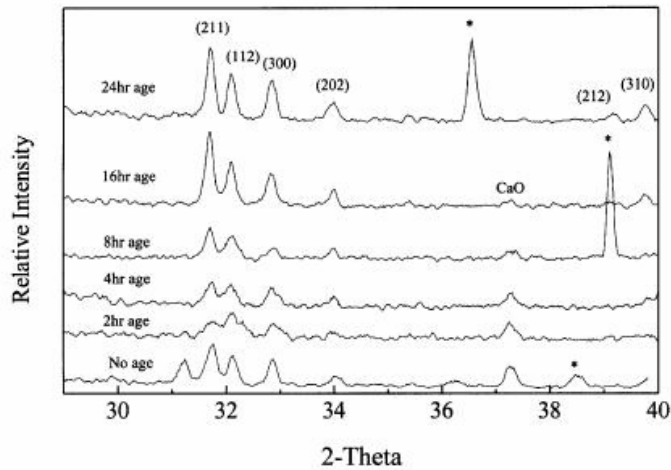


Fig. 1 X-ray diffraction data as a function of aging time. Peaks labelled with an asterisk represent Laue reflections from the single-crystal substrate. [14]

A significant increase in the peak intensity of the crystalline HA phase was observed in the XRD pattern. The peak of a secondary phase, calcium oxide (CaO), gradually disappeared upon aging. They also reported some other calcium compounds were found in the pattern with aging time less than 24 hr. The presence of these compounds indicates

the lack of the HA phase. But in their report, only aging time was discussed and aging temperature wasn't taken into account. Liu *et al.* [12] studied the aging effect on the formation of apatite phase in terms of both aging time and temperature. Their results show that aging time is considerably reduced as aging temperature increases. The XRD patterns of samples aged for different period time are shown in Fig. 2.

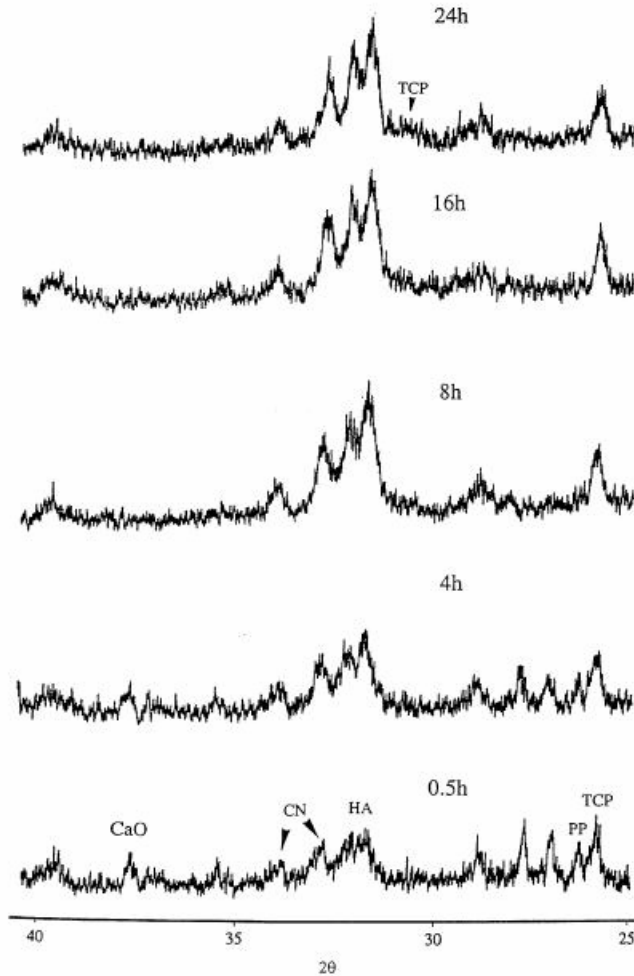


Fig. 2 XRD patterns of the gels, prepared from different aging time periods, after 400°C calcinations. Impure TCP phase appeared after aging for greater than 16 hr. (the abbreviation of PP: $\text{Ca}_2\text{P}_2\text{O}_7$, TCP: $\text{Ca}_3(\text{PO}_4)_2$, CN: $\text{Ca}(\text{NO}_3)_2 \cdot 4\text{H}_2\text{O}$ will also be used in other XRD diagrams in this work) [12].

For the case of 24 hr aging, calcined gels show the presence of small amount of β -tricalcium phosphate. They concluded that long term thermal aging was not favorable for apatite formation. Thermal aging was also studied. A phase evolution map was then

developed and shown in Fig 3. In this phase evolution map, the shadowed region between two curves indicates the optimum aging parameters for single-phase apatite formation. The final product obtained in the lower-bound region is accompanied by CaO while the product obtained in the upper bound region indicates the formation of secondary phases which was indicated in the figure. This phase evolution map is specified to a calcination temperature of 400°C.

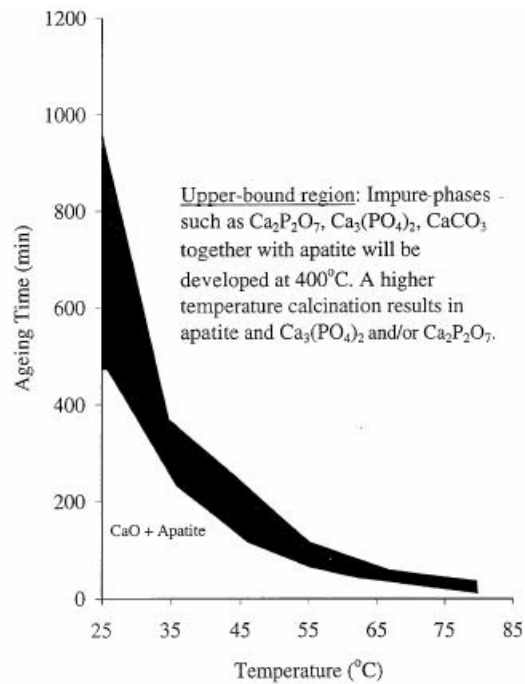


Fig. 3 Phase evolution map for apatite formation in terms of aging time and temperature [12].

2.1.3 Calcination

A crystallized phase of HA is formed upon calcination. The growth kinetics of HA formed from the dried gel was measured between 420°C to 550°C by Lopatin *et al.* [22]. They observed a rapid crystallization kinetic during the transition from the amorphous gel to crystallize HA at a temperature around 460°C. This temperature is then being considered as the transition temperature. Liu *et al.* [33] showed the XRD pattern of gels

calcined at different temperatures. The XRD patterns are shown in Fig. 4. They observed that the crystallized HA phase started to appear at a temperature as low as 350°C, which is lower than those reported in literature for alternative sol-gel routes to HA by 200 – 300°C [15,34].

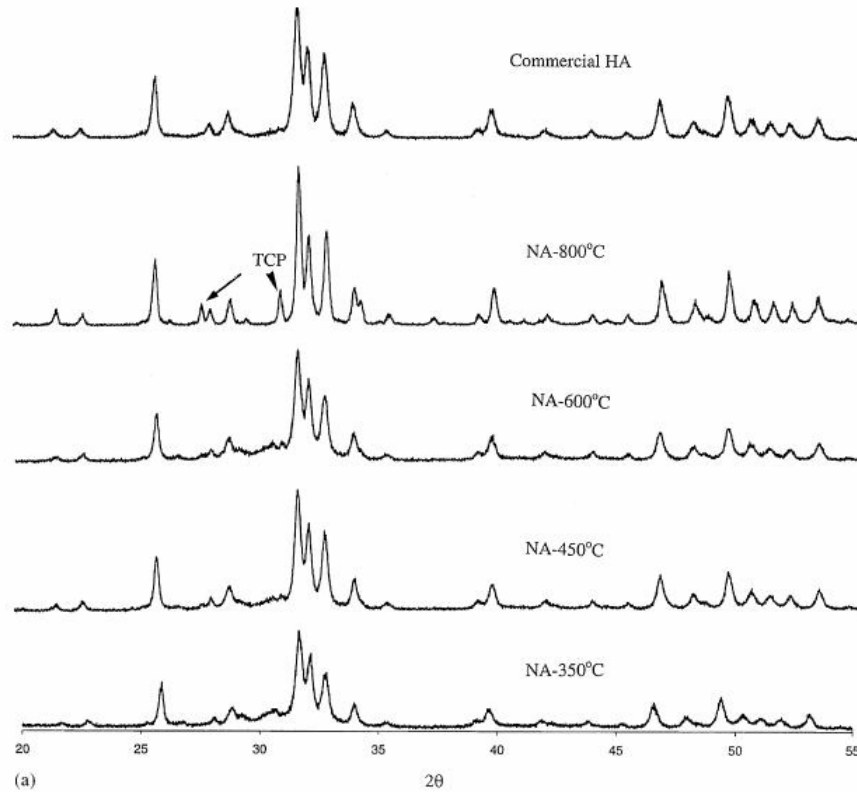


Fig. 4 XRD patterns for gel calcined at different temperatures. A predominant apatitic phase can be obtained, with a minor amount of TCP phase which developed at higher temperature. An XRD pattern (at the top in (a)) of commercial HA is also provided for comparison [13].

They also calculated the crystal size from the XRD pattern by using the Scherrer equation [34].

$$B = \frac{0.9\lambda}{t \cos \theta} \quad (1)$$

where B equals to FWHM (full width at half maximum) of the broadened diffraction line on the 2θ scale, which is the reflection of (002) plane, λ is the wavelength for Cu-K α (λ

=0.15418 nm) and t is the diameter of the crystallites. The data of Liu's [33] result were replotted in Fig. 5. The crystals increase from ~120 nm at 350°C to ~210 nm at 800°C. The inserted picture shows the SEM photograph of the gel calcined at 800°C. An average crystal size of 200nm was observed, which is close to the crystal size determined from the XRD analysis.

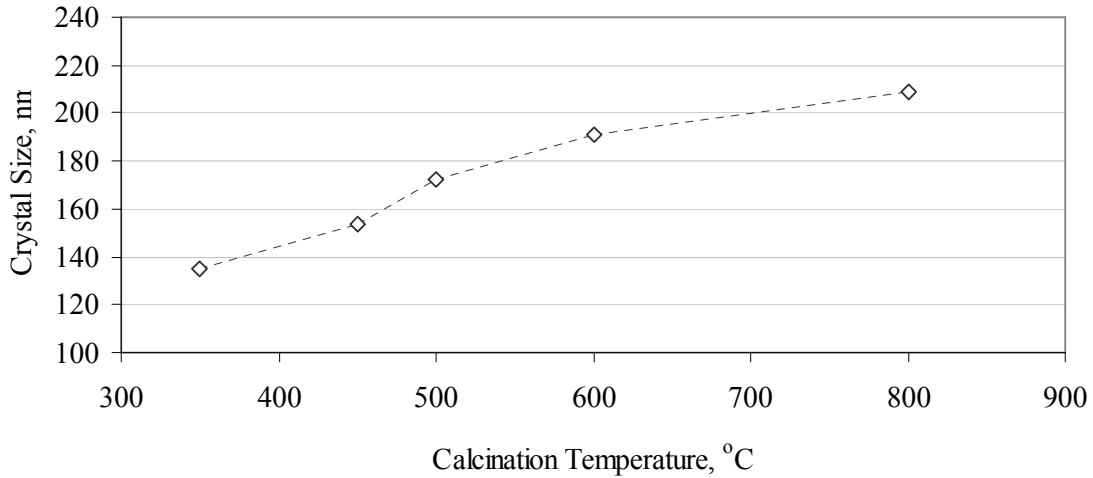


Fig. 5 Crystal size of the gels based on the Scherrer equation, calcined at different temperatures. The inset represents the SEM photograph of the microstructure for the gel calcined at 800°C; an average size of approximately 200 nm, in agreement with calcination, was observed. Some sintering behavior is also seen[33].

2.2 Electrospinning of Poly(vinyl alcohol)

Poly(vinyl alcohol) (PVA) is a semi-crystalline, hydrophilic polymer. Because of its high biocompatibility and non-toxic properties, PVA has been widely used in medical, cosmetic, and pharmaceutical fields. The high water permeability also makes it easy to be processed [31].

PVA is soluble in highly polar and hydrophilic solvents. Water is the most important solvent for PVA in many applications [24]. The viscosity of PVA solutions (η) depends

on the molecular weight (M_w), concentration (c), degree of hydrolysis, temperature (T) and the type of solvent. The dependence of zero shear viscosity on M_w in many polymers can be described by the following *Power law* equation [25]:

$$\eta = K'(M_w)^{3.4} \quad (3)$$

In general, the effects of M_w and c on solution viscosity can be modeled as [34]:

$$\eta = K(c\rho)^\alpha (M_w)^\beta \quad (4)$$

The measured viscosity data for PVA solutions in water [26] has been fitted to the above power law equation by Tao [28]. The exponents α and β were calculated to be 4.39 and 2.90, respectively. Equation (4) was then used to generate viscosity data for the molecular weights and concentrations used in this study as shown in Fig. 6 [28].

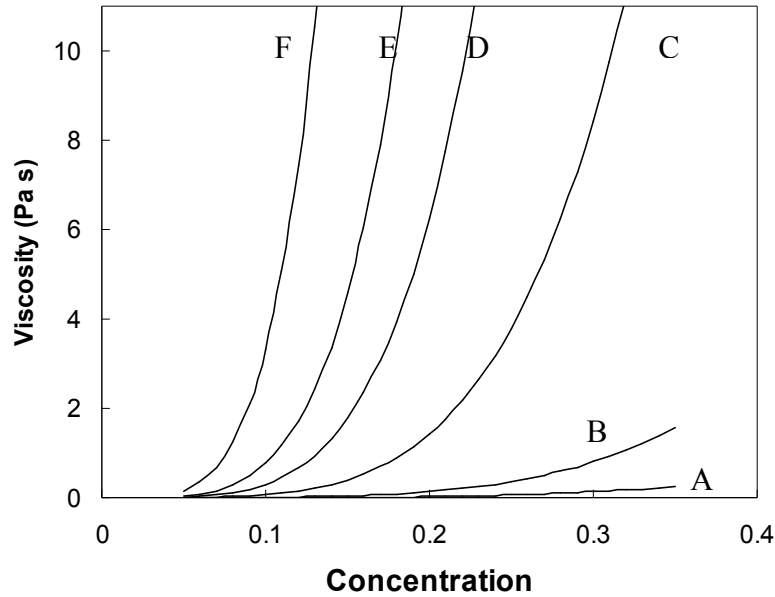


Fig. 6 Variation of solution viscosity with molecular weight and concentration. The measured viscosity data from the literature has been fitted to equation (4) [26]. This equation was then used to predict the viscosity for molecular weights and concentrations used in this study. The letters in the legend correspond to the PVA molecular weight (A) 9,500 g/mol; (B) 18,000 g/mol; (C) 40,500 g/mol; (D) 67,500 g/mol; (E) 93,500 g/mol; and (F) 155,000 g/mol [28].

The viscosity of the solution depends strongly on M_w and concentration. The intrinsic viscosity $[\eta]$ for polymer solutions can be related to M_w by the Mark-Houwink equation [27]:

$$[\eta] = K(M_w)^a \quad (5)$$

The Mark-Houwink constants (K and a) for PVA reported in the literature for various conditions are summarized in Table 1. The product of $[\eta]$ and c can be used to define the *Berry* number, $Be = [\eta]c$. The typical variation of $[\eta]c$ with c for three values of M_w and various values of c at which stable fibrous structures were obtained is plotted in Fig. 7. As can be expected, $[\eta]c$ increases with c for various molecular weights. As M_w increases, the slope of lines in Fig. 7 increases. This result suggests that M_w has a greater effect on the rheological properties of the solution than the concentration. It is reported by Koski *et al.*[31] for PVA with different molecular weights, a fibrous structure was stabilized above a minimum concentration, generally corresponding to $[\eta]c > 5$.

Table 1 Mark-Houwink constants for PVA solutions obtained from various sources in the literature.

Solvent	Mw (g/mol)	Temperature(°C)	K (10 ⁻⁴ dl/g)	a	Reference
Water	6x10 ³ < M < 160x10 ³	30	6.66	0.66	[29]
Water	6·10 ³ < M < 21·10 ³	25	2.0	0.76	[29]
Water	69·10 ³ < M < 690·10 ³	30	6.51	0.628	[30]
Water	86.8% hydrolysis	NA	8.00	0.58	[24]
Water	93.5% hydrolysis	NA	7.40	0.6	
Water	96.4% hydrolysis	NA	6.90	0.61	
Water	100 % hydrolysis	NA	5.95	0.63	

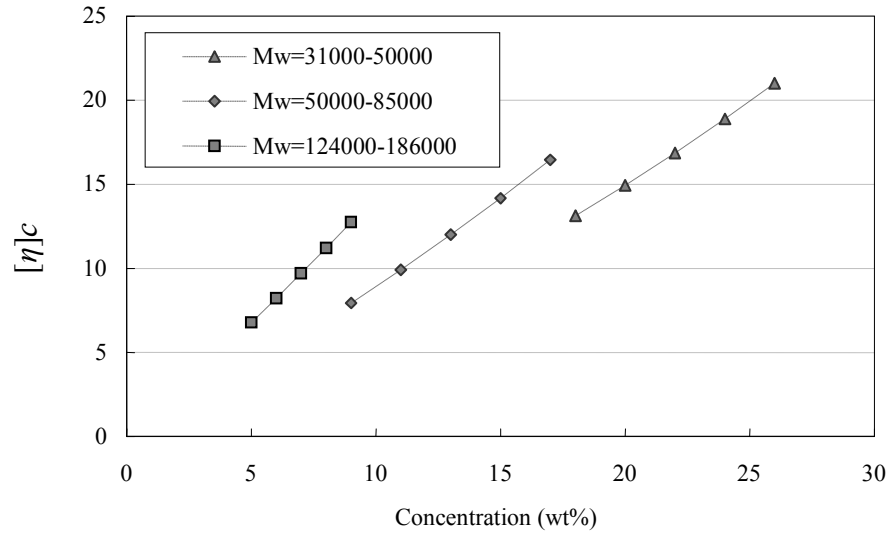


Fig. 7 Variation of Berry number $[\eta]c$ with the concentration of PVA in aqueous solutions. Data have been plotted for experimental conditions under which stable fiber structures were produced. The intrinsic viscosity has been calculated from the Mark-Houwink equation [34].

2.3 Electrospinning of ceramic fibers

Ceramic nanofibers synthesized via electrospinning were reported first in 2002 [36]; since then, various ceramic metal oxide fibers (with diameters between 200 and 400 nm) were obtained by high temperature calcination of the precursor organic-inorganic composite nanofibers assembled by electrospinning as shown in Figs. 8 and 9. Table 2 summarizes the featured systems to produce electrospun ceramic fibers. The materials being used and the featured characteristics are also shown in Table 2.

In a number of electrospun ceramic systems, a relatively long aging time is required to achieve the complete mixing between the polymer and the ceramic content. It was generally observed that the calcination temperature has a great influence on both the

crystalline phase and the surface morphology of the fibers. Larsen *et al.* [62] reported in the system of aluminum di-*sec*-butoxide ethylacetoacetate, which is used to prepare α - Al_2O_3 fibers, a 2 weeks' stabilization of the ready-to-spun sol was conducted at room temperature. The same group reported that, in order to produce silicon carbide, a 19 hr aging was at 65°C was necessary. Shao *et al.* [38] also reported a 12 hr mixing time is required to achieve the complete mixing between the polymer and ceramic precursors.

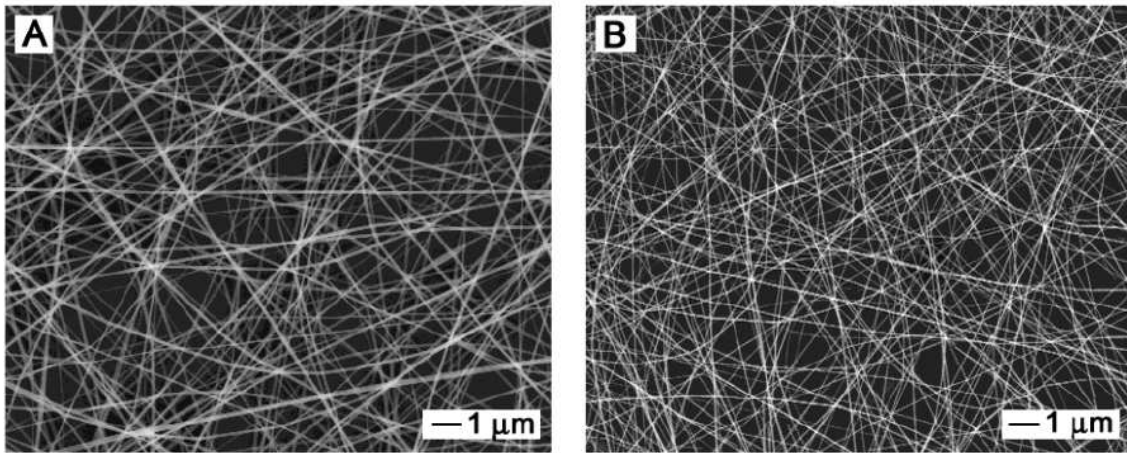


Fig. 8 (A) SEM image of TiO_2/PVP nanofibers that were electrospun from an ethanol solution containing $\text{Ti}(\text{OiPr})_4$ (0.1 g/mL) and PVP (0.03 g/mL). The electric field strength was 1 kV/cm. (B) SEM image of the same sample after it had been calcined in air at 500°C for 3 hr [43].

Many groups have reported that the morphologies of the final sample depend strongly on the calcination temperature. The dependence on calcination temperature is also linked to the nature of the target material. Viswanathamurthi *et al.* [41] reported a changing of the crystal structure in producing Niobium Oxide fibers by electrospinning upon calcination, as shown in Fig. 10.

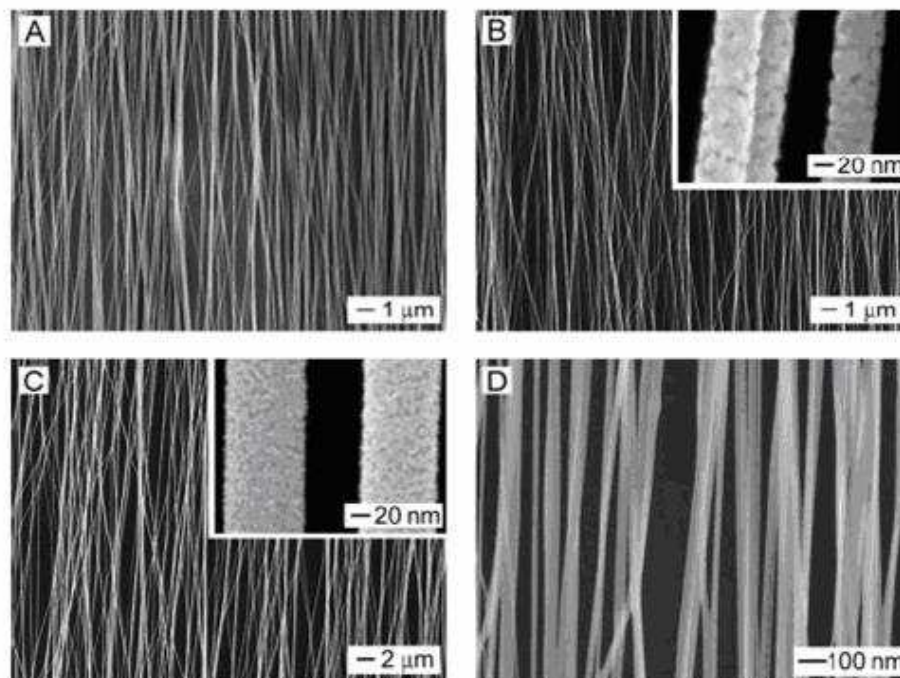


Fig. 9 SEM images of uniaxially aligned nanofibers made of different materials: a) TiO_2/PVP composite; B) polycrystalline TiO_2 ; C) polycrystalline, Sb-doped SnO_2 ; and D) polycrystalline NiFe_2O_4 . The insets show enlarged SEM images of the corresponding ceramic nanofibers [43].

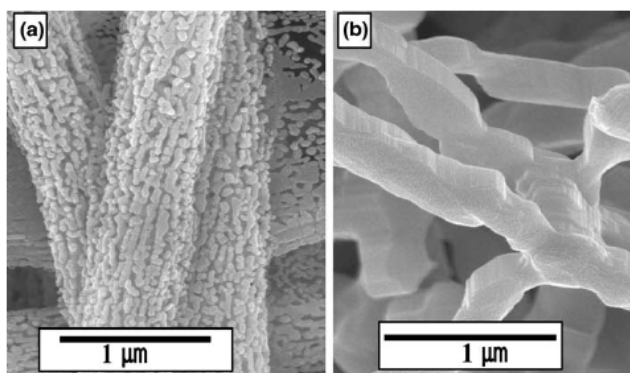


Fig. 10 SEM images of 50 wt% niobium oxide/PVAC fibers at high magnification: (a) calcined at 973 K, and (b) calcined at 1273 K [41].

In other systems, it is most likely that the crystalline phase is more pronounced with increasing the calcination temperature. As the X-Ray patterns in Fig. 11 show, Wang *et*

al [56] calcined tin oxide fibers in different temperatures. The fraction crystalline tin oxide increased with increasing of calcination temperature.

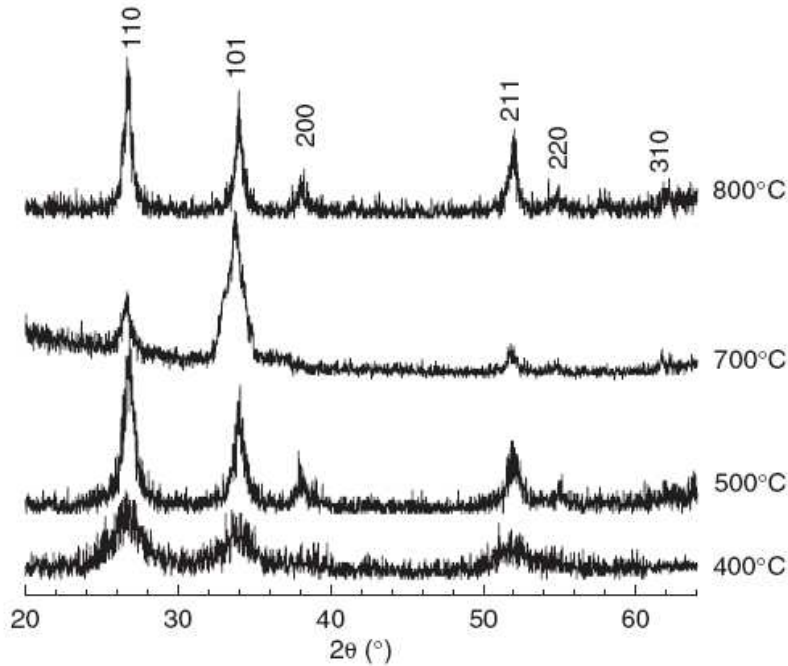
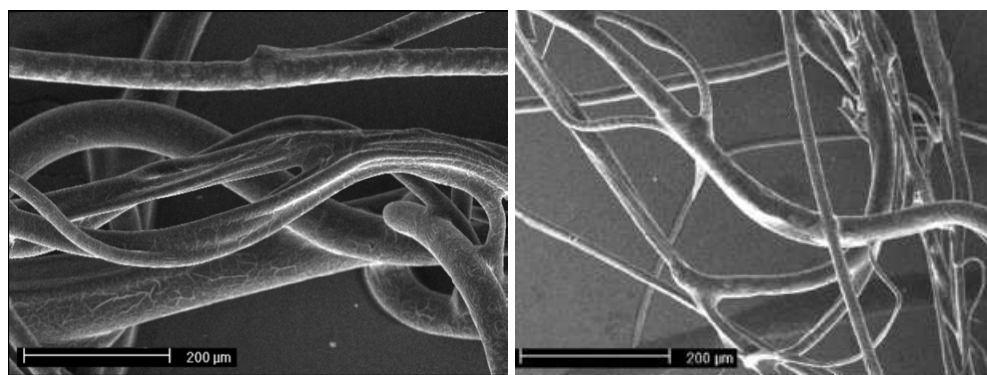


Fig. 11 X-ray diffraction spectra of tin oxide mats sintered at different temperatures [56].

Recently, Wu *et al.* [55] have produced HA fibers 10 to 30 μm in diameter by combining sol-gel processing with electrospinning. They used a precursor mixture of triethyl phosphite, calcium nitrite tetrahydrate and a polymer additive. After electrospinning and calcination at 600°C for 1 hr, HA fibers were obtained. The fiber diameters were in the order of 10~30 μm with a grain size of 1 μm , as shown in Fig. 12. Further developments in this structure should be focus on reducing the fiber diameter in order to fasten the resorption in the body.



(a)

(b)

Fig. 12 SEM photographs of the (a) as spun fiber, and (b) the calcined sample [55].

Table 2 Ceramic fibers via Electrospinning

Ceramic	Precursors	Method and Results	Reference
$\text{Al}_2\text{O}_3\text{-B}_2\text{O}_3$	<ol style="list-style-type: none"> 1. Aluminum acetate stabilized with boric acid ($\text{CH}_3\text{CO}_2\text{Al}(\text{OH})_2 \cdot \frac{1}{3}\text{H}_3\text{BO}_3$); 2. PVA with $M_n=86,000\text{g/mol}$; 3. Aqueous solution. 	$d \approx 550\text{ nm}$ Grain size increased with increasing calcination temperature. New phase form upon calcination. (Grain size = 41 nm at 1000°C . grain size with 82 nm at 1200°C)	36
Silica	<ol style="list-style-type: none"> 1. Tetraethyl orthosilicate (TEOS) $\text{Si}(\text{OCH}_2\text{CH}_3)_4$; 2. Distilled water, ethanol, and HCl. 	Sol was aged at 80°C for 30 min. No calcination is needed $d \approx 200\text{--}600\text{ nm}$	37
poly(vinyl alcohol)/silica composite	<ol style="list-style-type: none"> 1. PVA ($M_n=86,000$); 10wt. % 2. Tetraethoxysilane (TEOS); 3. Phosphoric acid as catalyst; 4. Distilled water was used as solvent. 	Aging under 60°C for 12h. The as-spun fiber mats were dried 12 h at 70°C under vacuum Characterized without firing $d \approx 200\text{--}400\text{ nm}$	38
Al_2O_3	<ol style="list-style-type: none"> 1. Aluminum di-sec-butoxide ethylacetoacetate; 2 Acidic $\text{H}_2\text{O}/\text{EtOH}$ media. 	$d < 200\text{ nm}$	39
Co_3O_4	<ol style="list-style-type: none"> 1. Cobalt acetate ($\text{Co}(\text{CH}_3\text{COO})_2 \cdot 4\text{H}_2\text{O}$) 2. PVA 3. Aqueous environment 	20g aqueous PVA solution of 10 wt. % + aqueous cobalt acetate solution (1.0 g $\text{Co}(\text{CH}_3\text{COO})_2 \cdot 4\text{H}_2\text{O}$ and 2.0 g H_2O); Aging at 50°C for 5 h.	40

		d \approx 50 – 200 nm.	
Nb ₂ O ₅	1. Niobium ethoxide 2. Acetic acid and ethanol 3. PVAC (14 wt.%) acetone solution.	Niobium ethoxide was dissolved in ethanol. Acetic acid was added as hydrolysis aid. Aged for 5 hr. d \approx 0.5 μ m	41
NiFe ₂ O ₄	1. iron(III) ethylhexano-isopropoxide 2. nickel ethylhexano isopropoxide 3. Isopropanol and acetic acid 4. PVP ($M_w=1,300,000$).	Reacted for 2 hr before electrospin hydrolysis after spinning d \approx 46 nm	42
TiO ₂	1. Titanium Tetraisopropoxide (Ti(OiPr) ₄ ; 2. poly(vinyl pyrrolidone) (PVP, $M_w \approx 1,300,000$); 3. Acetic acid; 4. Ethanol	1.5 g of titanium tetraisopropoxide (Ti(OiPr) ₄ , Aldrich) was mixed with 3 mL of acetic acid and 3 mL of ethanol; 0.45 g of PVP in 7.5 mL of ethanol solution; No long time aging.	43
Fe ₃ O ₄	1. Iron (II) chloride + iron (III) chloride + graft copolymer; 2. PEO or PVA	Initial co-precipitation reaction; No polymer burnout	44
Pb(Zr _{0.52} Ti _{0.48})O ₃	1. zirconium <i>n</i> -propoxide, 2. Titanium isopropoxide 3. Lead 2-ethylhexaonate 4. Xylene	D \approx 100-500nm	45
MgTiO ₃	1. Magnesium ethoxide 2. Titanium isopropoxide 3. 2-Methoxyethanol in N ₂ 4. Polyvinylacetate in DMF	Sol first, then polymer addition	46
NiTiO ₃	1. Nickel acetate 2. Ethanol 3. HNO ₃ 4. Titanium isopropoxide 5. Polyvinylacetate in DMF	Sol first, then polymer addition	47
ZrO ₂	1. Zirconium oxychloride (ZrOCl ₃) 2. Polyvinyl alcohol (PVA) Mn=80,000, 3. Aqueous environment	Aged at 60°C for 5 h. d \approx 50–200nm	48
NiCo ₂ O ₄	1. Co(CH ₃ COO) ₂ ·4H ₂ O; 2. Ni(CH ₃ COO) ₂ ·4H ₂ O;	electrospun fibers mats were dried initially 2 h at	49

	3. PVA aqueous solution (9.0 wt.%, Mn= 80,000), 4. Deionized water was used as the solvent.	90 °C under vacuum; No long time aging. d \approx 50–100 nm	
LiMn ₂ O ₄	1. Lithium chloride (LiCl·1H ₂ O) 2. Manganese acetate (Mn(CH ₃ COO) ₂ ·4H ₂ O) 3. Aqueous environment 4. PVA solution of 10 wt%	The electrospun fibers were dried initially 6 h at 70 °C under vacuum and then being fired; d \approx 100–200 nm.	50
GeO ₂	1. Germanium isopropoxide 2. PVAC 3. Acetone	Sol-gel; a-quartz like structure	51
Mn ₂ O ₃ –Mn ₃ O ₄	1. Manganese acetate (Mn(CH ₃ COO) ₂ ·4H ₂ O); 2. PVA with Mn=80,000, 3. Distilled water was used as solvent.	PVA aqueous solution of 10wt%; Aged 50°C for 5 h; d \approx 50–200nm.	52
TiO ₂	1. Titanium butoxide 2. P-123 (EO ₂₀ PO ₇₀ EO ₂₀) (BASF) 3. HCl	Sol-gel; mesoporous fibers	53
NiO/ZnO	1. Nickel acetate 2. Zinc acetate Fibers 3. PVA	Sol-gel; two phase ceramic	54
Ca ₁₀ (PO ₄) ₆ (OH) ₂	1. Ca (NO ₃) ₂ · 4H ₂ O; 2. (C ₂ H ₅ O) ₃ PO 3. polymer additive	Elelectrospinning and calcination at 600°C for 1 h	55
SnO ₂	1. Dimethyldineodecanoate tin (C ₂₂ H ₄₄ O ₄ Sn) 2. PEO 3. CHCl ₃	Simple precursor 100 mg. PEO + 10 ml CHCl ₃ Sol: Polymer = 1:2 d \approx Micro- to nano-fibres	56
	1. Anhydrous tin (IV) chloriline SnCl ₄ 2. Poly(ethylene oxide) (PEO) (Mn= 900 000) and and chloroform (CHCl ₃) 3. Deionized water, propanol (C ₃ H ₇ OH), isopropanol (2-C ₃ H ₇ OH)	Sol-gel SnCl ₄ :H ₂ O:C ₃ H ₇ OH:2-C ₃ H ₇ OH=1:9:9:6. 200 mg PEO + 10 ml CHCl ₃ Sol: Polymer = 1:1.25 d \approx 100 nm to several micrometers Different firing temperatures for 2hr	57
TiO ₂	1. Titanium isopropoxide 2. Polystyrene 3. Acetic acid	Sol-gel; nanofibers with core-sheath, hollow, or porous	58

	4. DMF–THF 5. PVP 6. Mineral Oil	structures; remove mineral oil to get hollow fibers; removal of PVP by calcinations makes hollow anatase nanofibers	
SiO ₂	1. Tetraethylorthosilicate 2. Ethanol 3. HCl	Sol–gel	59
BaTiO ₃	1. Barium acetate (Ba(CH ₃ COO) ₂) 2. Titanium isopropoxide [(CH ₃) ₂ CHO] ₄ 3. PVP (M _w =1,300,000) 4. Ethanol 5. Acetic acid environment for sol synthesis	PVA ethanol solution (PVP: 0.2 g and ethanol: 3 ml) d≈80 - 190 nm	60
CeO ₂	1. Cerium nitrate 2. PVA	PPT (co-precipitation) d≈50-150 nm	61

3. OBJECTIVES

The overall objectives of this work are to develop a suitable processing methodology to produce porous calcium phosphate scaffolds with properly controlled interconnectivity by using electrospinning in combination with the sol-gel technique. The specific goals are to:

- ◆ determine the processing conditions to produce predominantly hydroxyapatite after calcination
- ◆ study the effects of polymer molecular weight and sol volume fraction in the mixture on the electrospun structure
- ◆ examine the effects of calcination on the final structure